WAsP engineering flow model for wind over land and sea

Astrup, Poul; Larsen, Søren Ejling

Publication date:
1999

Document Version
Publisher's PDF, also known as Version of record

RISØ DK9901921

Risø-R-1107(EN)

WAsP Engineering Flow Model for Wind over Land and Sea

Poul Astrup, Søren E. Larsen

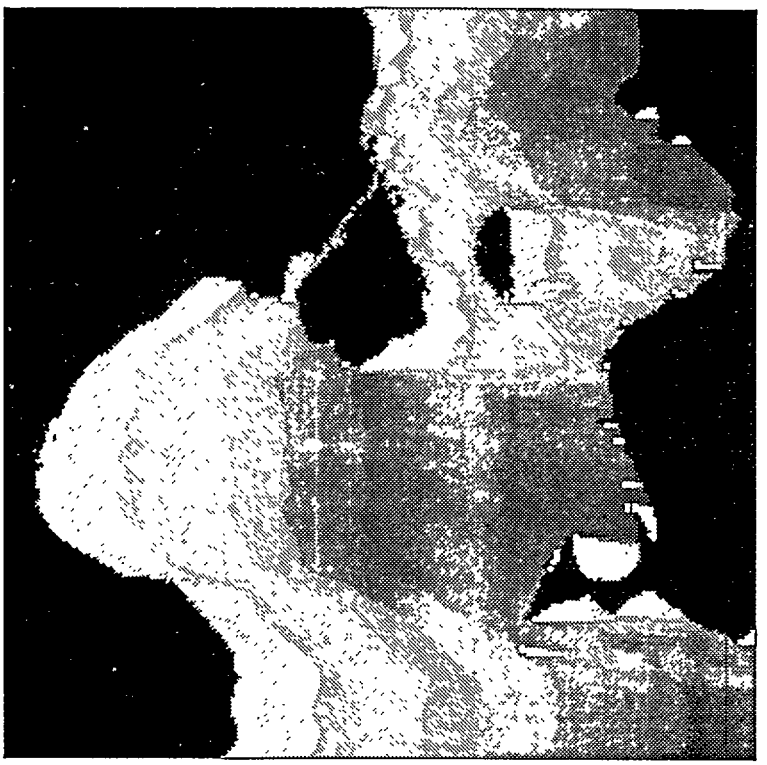

Risø National Laboratory, Roskilde, Denmark
August 1999

Risø-R-1107(EN)

WAsP Engineering Flow Model for Wind over Land and Sea

Poul Astrup, Søren E. Larsen

Risø National Laboratory, Roskilde, Denmark
August 1999

Abstract

This report presents the basic wind flow model of WAsP Engineering. The model consists in principle of three parts: the LINCOM model for neutrally stable flow over terrain with hills and varying surface roughness, a sea surface roughness model, and an obstacle model.

To better predict flow over or close to water bodies, the model for the sea surface roughness has been developed and interfaced with the existing LINCOM model. As the water roughness depends on the wind velocity, and the wind velocity on the roughness, the coupling is iterative.
The water roughness model is based on a fit to lots of literature data for the Charnock parameter as function of the so called wave age, the ratio between wave velocity and friction velocity, plus a correlation of wave age to the geometrically obtainable water fetch.

A model for the influence on the wind of multiple, finite size, interacting obstacles with any orientation has been formulated on the basis of the Perera formula for the influence of a single fence-like obstacle perpendicular to the wind. It is not a flow model but shall work as a postprocessor to the LINCOM model, which itself cannot treat such influence.

This project has been supported by the Danish Ministry of Environment and Energy under the Energy Research Program (ERP97), Journal No. 1363/97-0004.
The project partners are:
- Risø National Laboratory, Wind Energy and Atmospheric Physics Department;
- Svend Ole Hansen Aps.

ISBN 87–550–2529–3
ISSN 0106–2840

Information Service Department · Risø · 1999

Contents

Acknowledgements

We want to thank our colleague Helmut P. Frank for his great help with especially the water roughness model.

1 Introduction

WAsP Engineering is the title of a R&D project and a computer model, which has the objective to predict wind climate parameters of importance for the calculation of loads on wind turbines and other structures, onshore and in coastal waters.

The basic concept for WAsP Engineering comes from WAsP – the Wind Atlas Analysis and Application Program from Risø – which during the last decade has been used for wind resource estimation, wind data analysis and siting of wind turbines. A wind atlas contains – for each of e.g. 12 directional sectors – Weibull parameters for the mean wind at standard heights and roughnesses, and with such parameters for the region of interest, WAsP allows users to estimate the wind climate at specific locations, taking the relevant terrain effects into account.

WAsP Engineering extends the capability of WAsP to include the determination of wind parameters critical for loads and safety. It outputs profile data for mean and extreme winds plus turbulent conditions, and provides a simulated wind field as input to aeroelastic models.

The wind calculations of WAsP Engineering are performed with the LINCOM program, Astrup et al. 1996 [1], which is here interfaced with a module giving the sea surface roughness as function of wind speed and water fetch.
In contrast to the wind program of WAsP, which calculates the flow in a single point of interest, LINCOM calculates a flow field over an area. For a number of specified points of interest within this area the LINCOM results are extracted, and a postprocessor is applied to calculate the turbulence spectra, Mann 1999 [13]. Another postprocessor gives an estimate of the speed reduction caused by obstacles.
The calculations are based on wind atlas data for mean and extreme winds for the area in question together with information on orography, land roughness, and water fetch for the grid points of the calculational area.

This report describes the flow model of WAsP Engineering, i.e. the LINCOM model, the water roughness model, and the water fetch model. Finally it also contains a thorough description of the obstacle model.

2 The LINCOM flow model

Within the concept of linearized flow models originally introduced by Jackson and Hunt 1975 [8], Troen and de Baas 1986 [18] developed a relatively simple model for neutrally stable flow over hilly terrain. The model was later named LINCOM, an acronym for LINearized COMputation. Several investigators extended and changed the model in different ways until Santabàrbara et al. 1994 [16] rewrote it from scratch. The base of that version, giving the influence of the topography on the flow of a neutrally stable atmospheric layer, has been extended by Astrup et al. 1996 [1] with a model for the influence of varying surface roughness.

2.1 Linearized flow equations

Viewing the flow over a complex terrain as the sum of a main logarithmic profile flow over a flat terrain with uniform roughness and a field of perturbations caused by the departure from the flat terrain and uniform roughness, a steady state equation system for the perturbations can be deduced from the normal set of mass and momentum equations. And the assumption that these perturbations are small compared to the main flow makes linearization of the equations possible. The final set reads:

$$U\frac{\partial \widetilde{u}}{\partial x}+V\frac{\partial \widetilde{u}}{\partial y} = -\frac{\partial}{\partial x}\frac{\widetilde{p}}{\rho}+K_{xy}\left(\frac{\partial^2 \widetilde{u}}{\partial x^2}+\frac{\partial^2 \widetilde{u}}{\partial y^2}\right)+K_z\frac{\partial^2 \widetilde{u}}{\partial z^2} \quad (1)$$

$$U\frac{\partial \widetilde{v}}{\partial x}+V\frac{\partial \widetilde{v}}{\partial y} = -\frac{\partial}{\partial y}\frac{\widetilde{p}}{\rho}+K_{xy}\left(\frac{\partial^2 \widetilde{v}}{\partial x^2}+\frac{\partial^2 \widetilde{v}}{\partial y^2}\right)+K_z\frac{\partial^2 \widetilde{v}}{\partial z^2} \quad (2)$$

$$U\frac{\partial \widetilde{w}}{\partial x}+V\frac{\partial \widetilde{w}}{\partial y} = -\frac{\partial}{\partial z}\frac{\widetilde{p}}{\rho}+K_{xy}\left(\frac{\partial^2 \widetilde{w}}{\partial x^2}+\frac{\partial^2 \widetilde{w}}{\partial y^2}\right)+K_z\frac{\partial^2 \widetilde{w}}{\partial z^2} \quad (3)$$

$$\frac{\partial \widetilde{u}}{\partial x}+\frac{\partial \widetilde{v}}{\partial y}+\frac{\partial \widetilde{w}}{\partial z} = 0 \quad (4)$$

Here $(U,V,0)$ is the main unperturbed flow vector, $(\widetilde{u},\widetilde{v},\widetilde{w})$ the velocity perturbation vector, and $\widetilde{p}$ the pressure perturbation. The K's are the effective kinematic viscosities in horizontal and vertical directions, subscript xy and z respectively.

2.2 Solution method

The solution method is spectral i.e. the mass and momentum equations are rewritten in terms of the Fourier transforms of the dependent variables.

Taking the Fourier transform over the two horizontal coordinates, the differential x and y dependencies transform to scalar dependencies on the corresponding wave numbers k and m, leaving differential dependence only on the z coordinate.
Keeping the main flow vector and the viscosities independent of position the Fourier domain mass and momentum equations equivalent to those of the above set become:

$$(ikU+imV)\,u = -ikp-K_{xy}(k^2+m^2)\,u+K_z\frac{\partial^2 u}{\partial z^2} \quad (5)$$

$$(ikU+imV)\,v = -imp-K_{xy}(k^2+m^2)\,v+K_z\frac{\partial^2 v}{\partial z^2} \quad (6)$$

$$(ikU+imV)\,w = -\frac{\partial p}{\partial z}-K_{xy}(k^2+m^2)\,w+K_z\frac{\partial^2 w}{\partial z^2} \quad (7)$$

$$iku+imv+\frac{\partial w}{\partial z} = 0 \quad (8)$$

Here u, v, w, and p are the Fourier transforms of $\widetilde{u}$, $\widetilde{v}$, $\widetilde{w}$, and $\widetilde{p}/\rho$.
These equations have analytical solutions of the form

$$a = \sum_i a_{i0}\,e^{\alpha_i z} \quad (9)$$

which introduced into eqs. 5 to 8 and with

$$C \equiv i(kU + mV) + K_{xy}(k^2 + m^2) - K_z\alpha^2 \tag{10}$$

yields the matrix equation

$$\begin{pmatrix} C & 0 & 0 & ik \\ 0 & C & 0 & im \\ 0 & 0 & C & \alpha \\ ik & im & \alpha & 0 \end{pmatrix} \begin{pmatrix} u \\ v \\ w \\ p \end{pmatrix} = \begin{pmatrix} 0 \\ 0 \\ 0 \\ 0 \end{pmatrix} \tag{11}$$

This obviously has the uninteresting solution $(u, v, w, p) = \mathbf{0}$, so interesting solutions are only found when the matrix has zero determinant. This means

$$C^2(k^2 + m^2 - \alpha^2) = 0 \tag{12}$$

which leads to the applicable α's. For the solutions to stay limited for increasing z only α's with a negative real part have reason and the possible values corresponding to $C \neq 0$ and $C = 0$ respectively become:

$$\alpha_1 = -\sqrt{k^2 + m^2} \tag{13}$$

$$\alpha_2 = -\left[\frac{(kU + mV)^2 + K_{xy}^2(k^2 + m^2)^2}{K_z^2}\right]^{\frac{1}{4}} \left(\cos\frac{\beta}{2} + i\sin\frac{\beta}{2}\right) \tag{14}$$

where

$$\beta = \arctan\frac{kU + mV}{K_{xy}(k^2 + m^2)} \tag{15}$$

Defining the outer and the inner length scales, L and l, and the numbers c and s

$$L \equiv \frac{1}{\sqrt{k^2 + m^2}} \tag{16}$$

$$l \equiv \left[\frac{(kU + mV)^2 + K_{xy}^2(k^2 + m^2)^2}{K_z^2}\right]^{-\frac{1}{4}} \tag{17}$$

$$c \equiv \cos\frac{\beta}{2} \tag{18}$$

$$s \equiv \sin\frac{\beta}{2} \tag{19}$$

the α's are expressed

$$\alpha_1 = -\frac{1}{L}$$

$$\alpha_2 = -\frac{c + is}{l} \tag{20}$$

The solution then becomes

$$\begin{pmatrix} u \\ v \\ w \\ p \end{pmatrix} = \begin{pmatrix} u_{10} \\ v_{10} \\ w_{10} \\ p_{10} \end{pmatrix} e^{-\frac{z}{L}} + \begin{pmatrix} u_{20} \\ v_{20} \\ w_{20} \\ p_{20} \end{pmatrix} e^{-(c+is)\frac{z}{l}} \tag{21}$$

where the first part is called the outer solution and the second part the inner solution. The components of the two amplitude vectors are subject to the following relations:

$$p_{10} = \left[i(kU+mV)L + (K_{xy}-K_z)L^{-1}\right] w_{10} \quad (22)$$

$$u_{10} = -ikLw_{10} \quad (23)$$

$$v_{10} = -imLw_{10} \quad (24)$$

$$iku_{20} + imv_{20} - \frac{c+is}{l} w_{20} = 0 \quad (25)$$

$$p_{20} = 0 \quad (26)$$

This leaves three degrees of freedom for the amplitude vectors for which reason three boundary conditions are needed to define the solution.

2.3 Spectral inner length scale

The derivation of the Fourier space equations relied upon the main flow vector $(U,V,0)$ and the effective kinematic viscosities K_{xy} and K_z all being constant in space. But for the determination of the inner length scale l their variation with height is anyway taken into account:

$$\begin{pmatrix} U \\ V \end{pmatrix} = \frac{U_*}{\kappa} \ln \frac{l\,c_1}{z_{00}} \begin{pmatrix} \cos\theta \\ \sin\theta \end{pmatrix} \quad (27)$$

$$K_{xy} = K_z = \kappa U_* l\, c_2 \quad (28)$$

Here θ is the wind direction angle, z_{00} is the mean roughness height over the calculational area. c_1 and c_2 are two model parameters of order unity which have been fixed from fitting to experiments. The definition of l, see eq. 17, together with these equations determine l's dependence upon the wave numbers k and m.

2.4 The hill model

Modelling perturbations caused by some flow disturbing phenomena is with LINCOM a question of applying appropriate boundary conditions for the above solution. For the perturbations caused by hills Troen and de Baas 1986 [18] applied the main condition that near the ground surface the flow shall be parallel to this. They used scale arguments to reduce this to a condition for the outer solution only, a "full slip" condition reading:

$$\widetilde{w}_{1,z=0} = U\frac{d\widetilde{h}}{dx} + V\frac{d\widetilde{h}}{dy} \quad (29)$$

where $\widetilde{h}$ is the ground surface elevation. The Fourier space equivalent reads:

$$w_{10} = i(kU+mV)h \quad (30)$$

h is the Fourier transform of $\widetilde{h}$, and (U,V) is here modelled following eq. 27 but with the inner length scale l replaced by the outer length scale L.
The remaining two boundary conditions are used to specify zero Fourier space horizontal velocity components at the surface.

2.5 The roughness model

The boundary conditions used for modelling the perturbations caused by roughness changes are derived from the hypothesis that near the ground, i.e. below a certain height z_r, the flow is in equilibrium with the local surface roughness:

$$\overline{v} = \begin{pmatrix} \cos\theta \\ \sin\theta \end{pmatrix} \frac{U_*}{\kappa} \ln\frac{z}{z_0} \tag{31}$$

where again θ is the wind direction angle, and U_* and z_0 are the local values of friction velocity and roughness length.
Defining the mean surface rouhgness z_{00} of the area as

$$\ln z_{00} \equiv \frac{1}{A}\int_A \ln z_0 \, dA \tag{32}$$

and specifying the local relative roughness η and the local friction velocity perturbation u_* from

$$\eta \equiv \frac{z_0}{z_{00}}$$

$$u_* \equiv U_* - U_{*0} \tag{33}$$

where U_{*0} is the mean friction velocity, i.e. that giving the main logarithmic profile over the flat terrain with invariable roughness z_{00}, then subtraction of the main flow from the local flow plus application of the assumption that $u_* \ll U_{*0}$ reveals an equation for the perturbed velocity which at height $z = z_r$ forms the real space boundary condition:

$$\widetilde{v} = \begin{pmatrix} \cos\theta \\ \sin\theta \end{pmatrix} \left(\frac{u_*}{\kappa} \ln\frac{z}{z_{00}} - \frac{U_{*0}}{\kappa} \ln\eta \right) \tag{34}$$

Together with

$$\frac{\partial \widetilde{v}}{\partial z} = \begin{pmatrix} \cos\theta \\ \sin\theta \end{pmatrix} \frac{u_*}{\kappa z} \tag{35}$$

this leads to the Fourier space boundary condition

$$\begin{pmatrix} u \\ v \end{pmatrix}_{z_r} = z_r \ln\frac{z_r}{z_{00}} \frac{\partial}{\partial z}\bigg|_{z_r} \begin{pmatrix} u \\ v \end{pmatrix} - \begin{pmatrix} \cos\theta \\ \sin\theta \end{pmatrix} \frac{U_{*0}}{\kappa} F[\ln\eta] \tag{36}$$

where $F[\,]$ indicates the Fourier transform of the applicable field.
Fourier transforming eq. 35 and introducing the solution for $(u,v)_{z_r}$ to this leads to an equation for the friction velocity perturbation:

$$F[u_*] = z_r U_{*0} F[\ln\eta] \frac{c+is}{l} \left[1 + z_r \frac{c+is}{l} \ln\frac{z_r}{z_{00}} \right]^{-1} \tag{37}$$

The resulting perturbation fields depend on the choice of z_r, the selection of which has therefore been based on tests against experiments. The actual expression which has been influenced by Frank 1996 [4] and Lange 1997 [12] reads:

$$z_r = 0.3\, z_{00}^{0.33} L_d^{0.67} \tag{38}$$

$$L_d = \frac{1}{|k\cos\theta + m\sin\theta|} \tag{39}$$

$$L_d \leq \frac{N\Delta x}{2\pi} = \frac{1}{k_1} \tag{40}$$

where k_1 is the smallest positive value of the wave number k, N the number of grid points, and Δx the x-direction grid size. The limiting of L_d is needed for numerical reasons.
The expression for z_r but with L_d replaced by the direction independent outer length scale L: $0.3 z_{00}^{0.33} L^{0.67}$ is originally proposed by N.O. Jensen 1984 [9] as a measure for the inner length scale l. N.O. Jensen also originated the idea of modelling the influence of varying roughness using a spectral method.

2.6 Final flow solution

To first order accuracy the perturbation fields caused by the two treated mechanisms do not influence each other and can therefore be solved for independently. The final flow field is then obtained by summing the two analytically found Fourier space perturbation fields, transferring the result into real space using a Fast Fourier Transform routine, and adding the outcome of this to the main flow field.

Figure 1 compares the results of the hill model – and hill plus roughness model – when applied to the terrain of the Askervein Hill with on site measurements.

Figure 2 compares the results of the roughness model with data from Bradley 1968 [2] and Peterson et al. 1979 [15].

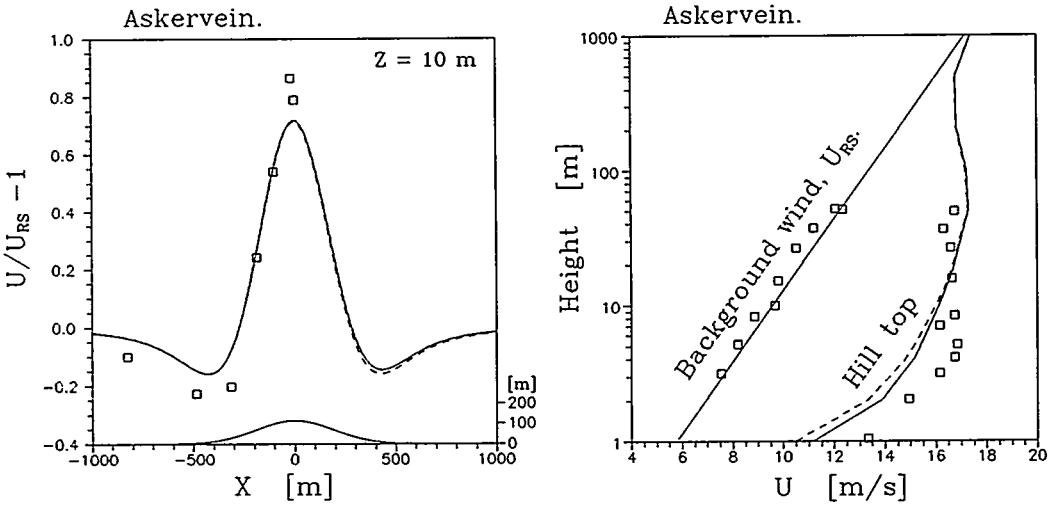

Figure 1. Askervein Hill test.
Left: Horizontal profiles of relative wind speedup 10 m above ground plus hill profile.
Right: Vertical profiles of wind speed. RS: Reference station.
Calculations: Full line: varying roughness. Dashed line: constant roughness. Squares indicate measurements.

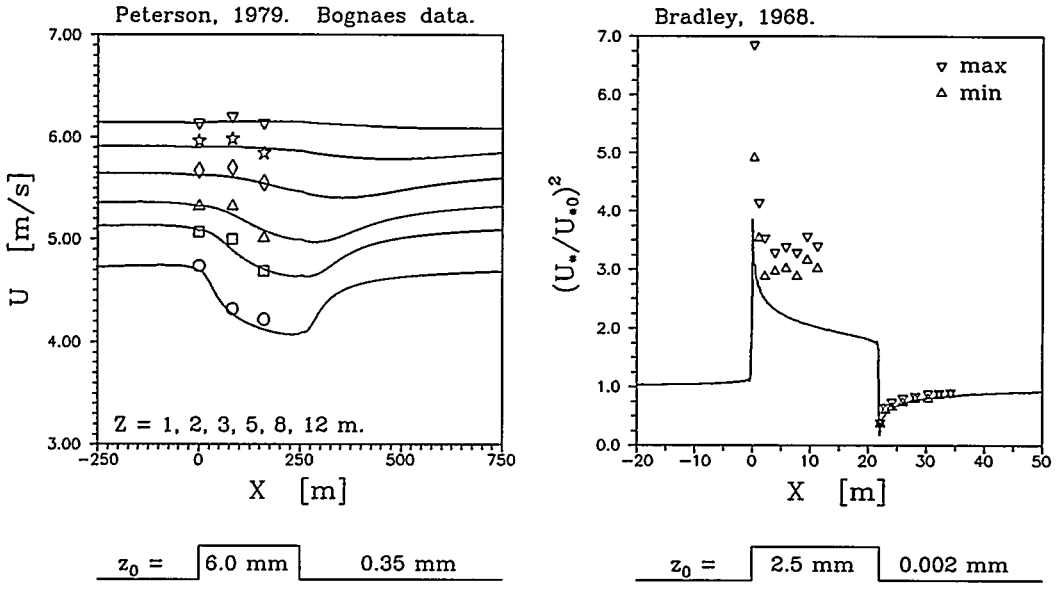

Figure 2. Left: Horizontal wind speed profiles at different heights over a roughness change. Data of Peterson et al. 1979 [15].
Right: Friction velocity profile over roughness changes. Data of Bradley 1968 [2].

3 Water roughness

For WAsP Engineering, the best possible prediction of flow over water bodies is of importance. For that reason a water roughness model i.e. a model giving the sea surface roughness height, has been interfaced with LINCOM. The modelled roughness depends upon the LINCOM calculated velocity field which in turn depends upon the modelled roughness. Reasonably consistent fields of roughness length and wind velocity are therefore obtained by iteration.
The term reasonable above indicates that the integration with LINCOM is through the velocity field only. The water roughness model assumes a purely logarithmic velocity profile

$$U = \frac{U_*}{\kappa} \ln \frac{z}{z_o} \tag{41}$$

so the U_* field calculated from this model and that of LINCOM's roughness (response) model may deviate.

The base of the model is the well known formula of Charnock 1955 [3] for surface roughness of the sea

$$z_o = A_c \frac{U_*^2}{g} \tag{42}$$

where Charnock's constant for open sea $A_c = 0.011$. Many investigators have found this constant not to be a real constant but depend upon wind as well as wave conditions. According to Johnson et al. 1998 [10]

$$A_c = 1.89 \left(\frac{U_*}{c}\right)^{1.59} \tag{43}$$

c being the speed of the waves, while Hansen and Larsen 1997 [5] for larger values of U_*/c find

$$A_c \propto \left(\frac{U_*}{c}\right)^{-2} \tag{44}$$

Toba et al. 1990 [17] find that

$$A_c = 0.025 \left(\frac{U_*}{c}\right)^{-1} \tag{45}$$

correlates a high number of measurements, and that the positive exponent as seen above in Johnson's formula may be a consequence of the wind fluctuating much more rapidly than the wave energy, i.e. on a short time scale the variation of A_c can follow an expression like that of Johnson but that describes variations around a "mean" given by eq. 45.
Højstrup 1997 [7], however, finds the formula of Johnson to correlate well with his roughness data for different sites and over a wide range of wind strength, and the model applied to LINCOM combines the model of Johnson with that of Toba et al. using the Johnson approach for values of U_*/c around 0.1, the $(U_*/c)^{-1}$ behavior up around $U_*/c = 1.0$ and $(U_*/c)^{-3}$ for even higher values, the latter solely to avoid numeric problems. The final correlation reads

$$A_c = 1.89 \left(\frac{U_*}{c}\right)^{1.59} \left[1.0 + 47.165 \left(\frac{U_*}{c}\right)^{2.59} + 11.791 \left(\frac{U_*}{c}\right)^{4.59}\right]^{-1} \tag{46}$$

Figure 3 shows this correlation together with the data used to fix the denominator constants. The data are from Johnson et al. 1998 [10] and from many others, but here taken from the paper of Toba et al. 1990 [17]. The figure also shows the correlation of Toba et al. 1990 [17], eq. 45
For small values of U_*/c the higher of eq. 46 and Charnock's open sea constant 0.011 is used.

The wave speed c is inaccessible but Hasselman et al. 1973 [6], among others, correlate the wave speed with the geometrically determinable fetch over water. Hasselman's expression reads

$$\left(\frac{U_*}{c}\right) = \frac{3.5}{2\pi} \left(\frac{U_{10}^2}{x\,g}\right)^{\frac{1}{3}} \tag{47}$$

where U_{10} is the wind speed at 10 m height and x is the water fetch. But even the water fetch may be inaccessible. Due to the limited calculational area water bodies may well reach the edge, so for certain ranges of wind directions smaller or larger parts of the water grid points may have no defined upstream coastline. In that case open water is assumed and Charnock's formula, eq. 42, is used.

As a final step it is checked if the found roughness is smaller than that corresponding to a smooth surface as given by

$$z_o = \frac{\nu}{9.025\,U_*} \tag{48}$$

in which case the smooth surface value is used.

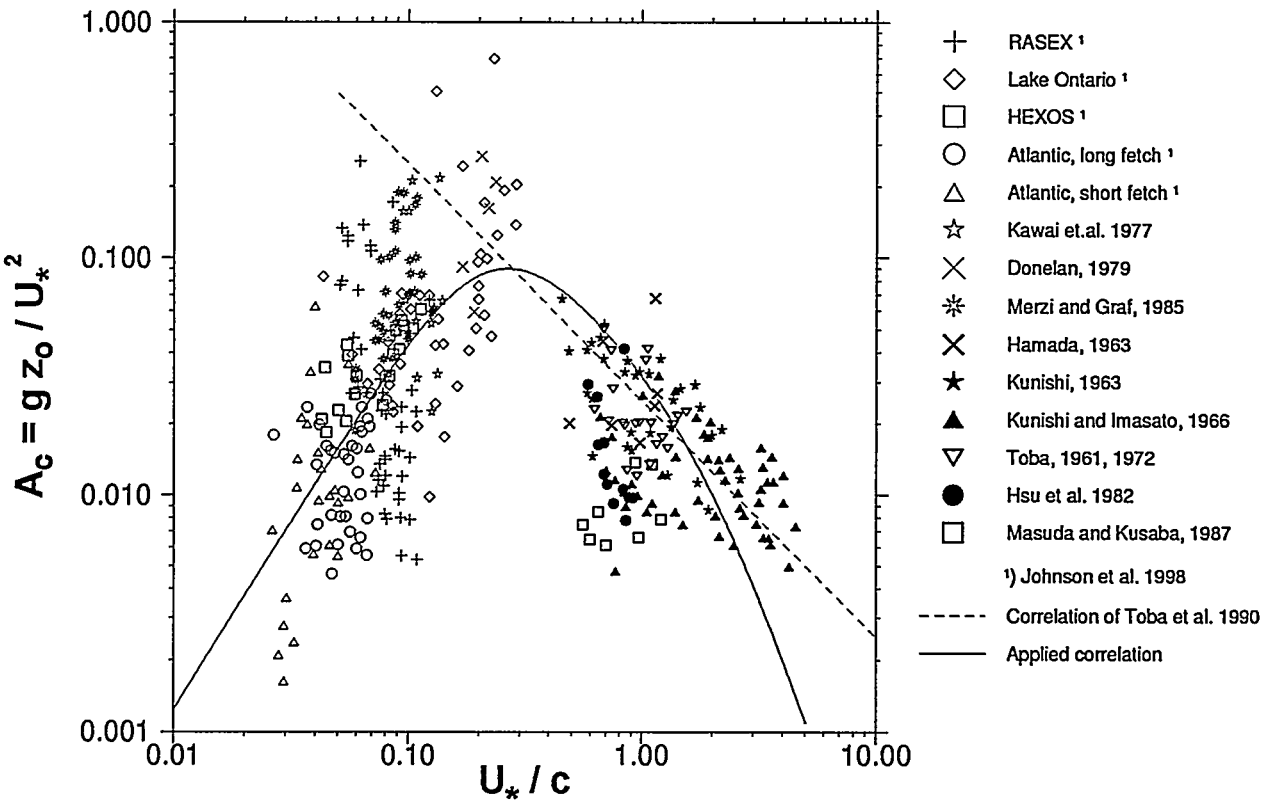

Figure 3. Comparison of eqs. 46 and 45 to data.

4 Fetch over water

As required input for the water roughness model, the fetch over water has to be derived for every water point of the calculational grid.

With simple water fetch defined as the distance directly against the wind from the actual grid point to the nearest upstream coastline, a small island in the middle of the ocean causes a narrow strip of reduced fetch all way to the horizon and below. With the roughness model strictly dependent on the calculated fetch, all resulting fields also show a narrow strip all way out to where Charnock friction takes over.
This is physically unreasonable but can not really be catered fore in the water roughness model, which in reality is a point model applied individually at every water grid point. In stead the fetch model is modified to not give the simple fetch but the mean of a number of simple fetches derived over a small range of wind directions centering on the specified direction.

The coastline information is obtained from a WAsP MAP file, where it is given as a succession of shorter or longer pieces of straight line. In the simple fetch calculation it's for every such shoreline piece calculated which water grid points are downstream of it, and the fetch for those points are then derived. Water grid points with no upstream coastline are finally given the value -1 as an indicator to the program using the fetch information that no fetch is obtainable.

In finding the mean of a number of simple fetches calculated for slightly different wind directions, problems arise with points for which part of the simple fetches are given as -1, this being a useless value for the mean derivation. As the -1 indicates the use of Charnock friction it has to be replaced by a fetch that gives Charnock friction, and as this fetch is used to generate a mean together with smaller fetches, it should be the minimum fetch giving Charnock friction.

Combining Johnson's formula, eq. 43, with Hasselman's, eq. 47, and using $A_c = 0.011$, the sought fetch x can be extracted as:

$$x = 2850 \frac{U_{10}^2}{g} \tag{49}$$

It just remains to find U_{10}.

The input wind to the flow part of WAsP Engineering is specified as speed U_s and direction D_s at height z_s over a terrain with roughness height z_{0s}, index s meaning specified. The logarithmic profile gives

$$U_{*s} = \frac{\kappa U_s}{\ln\left(\frac{z_s}{z_{0s}}\right)} \tag{50}$$

and the geostrophic law gives

$$G = \frac{U_{*s}}{\kappa} \sqrt{\left(\ln\left(\frac{U_{*s}}{f\, z_{0s}}\right) - A\right)^2 + B^2} \tag{51}$$

Here f is the Coriolis parameter, $A = 1.8$, and $B = 4.5$. Hereby G is known. Insertion of Charnock's formula, eq. 42, in the geostrophic law gives for a water point

$$G = \frac{U_*}{\kappa} \sqrt{\left(\ln\left(\frac{g}{f\, A_c\, U_*}\right) - A\right)^2 + B^2} \tag{52}$$

With $A_c = 0.011$, all is known except U_* which is then found by iteration. z_o then comes from Charnock's formula, eq. 42, and U_{10} from the logarithmic profile, and the searched minimum Charnock fetch from eq. 49. To put no more constraints than needed into the calculated fetch, the points finally getting a mean fetch equal to the found minimum Charnock fetch have this replaced with the -1 indicator, as the final flow solution may end at a slightly different fetch value for transition to Charnock friction than the one found here.

Figure 4 shows the difference between the simple fetch behind a small island, and the mean fetch over 11 degree behind the same island. For both pictures the -1 indicators have been exchanged with the minimum Charnock fetch for better visualization.

5 The obstacle model "Shelter"

The objective of the obstacle model is to predict the influence of upstream obstacles upon the wind speed in the points of interest.

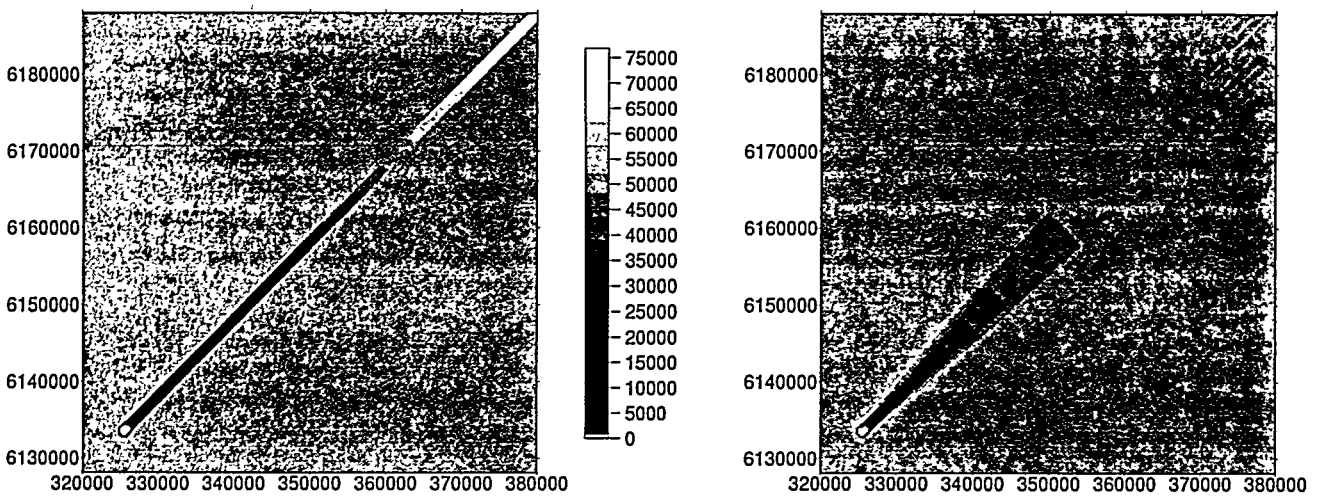

Figure 4. Left) Simple fetch behind island. Right) Mean fetch over 11 degree.

The obstacle model of WAsP Engineering is named "Shelter" and follows to a large extend the obstacle model of the previous WAsP model. Like that, it is based solely upon the correlation of Perera 1981 [14] plus some reasoning. It gives a rough estimate of the influence of obstacles. It is not a flow model.

The Perera formula is assumed valid behind a single infinitely long but thin obstacle – a fence – which is perpendicular to the direction of the wind. Real obstacles – needless to say – can have any form, can have the wind coming from any angle, and can stand in each others wind shadow.

The Perera formula, here taken from Landberg 1994 [11], reads

$$Pe = -\frac{\Delta U_z}{U_h} = 9.75(1-Po)\frac{h}{x}\eta \exp\left(-0.67\eta^{1.5}\right) \tag{53}$$

$$\eta = \frac{z}{h}\left(K\frac{x}{h}\right)^{\frac{-1}{n+2}} \tag{54}$$

$$K = \frac{2\kappa^2}{\ln\frac{h}{z_o}} \tag{55}$$

x	distance downstream obstacle [m]
U_h	free wind speed [m/s] in obstacle height h
n	velocity profile exponent ($n = 0.14$)
h	height of obstacle minus zero displacement [m]
Po	porosity of obstacle (0: solid, 1: no obstacle)
z	height [m] for which the velocity deficit is calculated
z_o	roughness height [m]

Figure 5 shows $-\Delta U_z/U_z$ as function of x/h and z/h for $h/z_o = 100$, obtained by multiplying the found $\Delta U_z/U_h$ from eqs. 53, 54, 55, with the free stream velocity ratio $U_h/U_z = (h/z)^n$. Studying this figure it is clear that for small values of x/h, the Perera formula is far from reality: at any height $Pe \to 0$ for $x \to 0$, and the reverse flow bubble has no good dimensions.

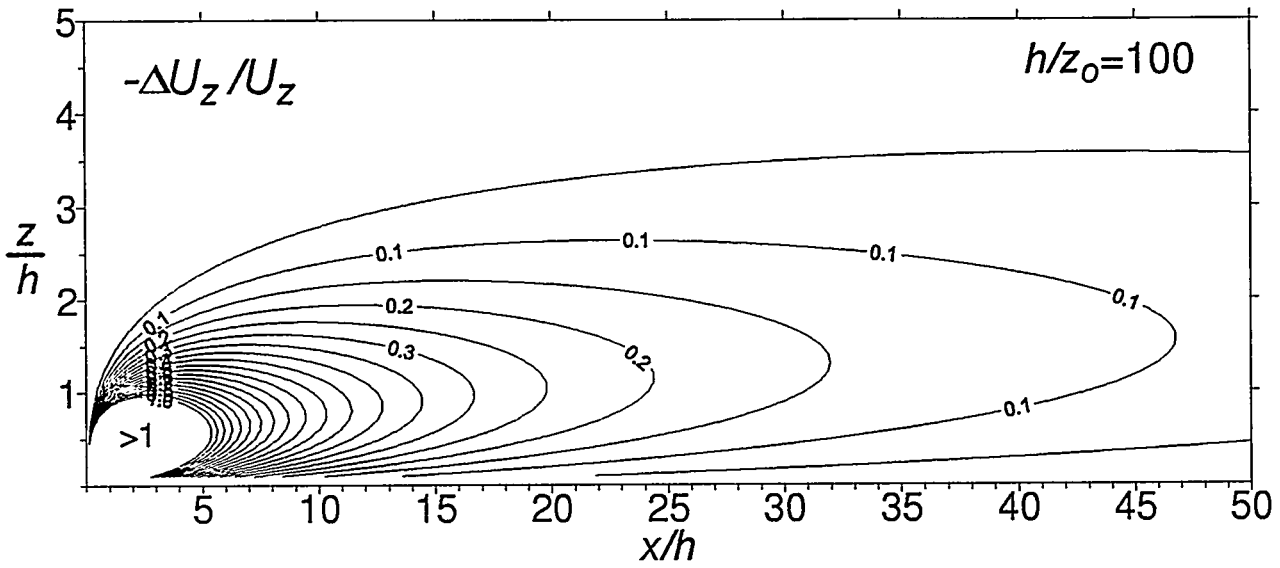

Figure 5. Perera's formula for $-\Delta\, U_z/U_z$ as funtion of x/h and z/h.

5.1 Finite obstacle length

As a first step towards a model for real obstacles the behaviour of a finite length thin obstacle perpendicular to the wind is sought. It is reasonable to think that at great distance the influence of a continuous obstacle with a certain porosity equals the influence of a series of solid interspaced obstacles.
Figure 6 shows such a series of obstacles. If the influence at the point marked at distance x behind the obstacle is the sum of influence of all the individual obstacles, this influence must decrease for obstacles at numerically increasing angle α. Introducing a geometrical distribution function $f(x,y)$ fulfilling

$$1 = \int_{-\infty}^{\infty} f(x,y)\, dy \tag{56}$$

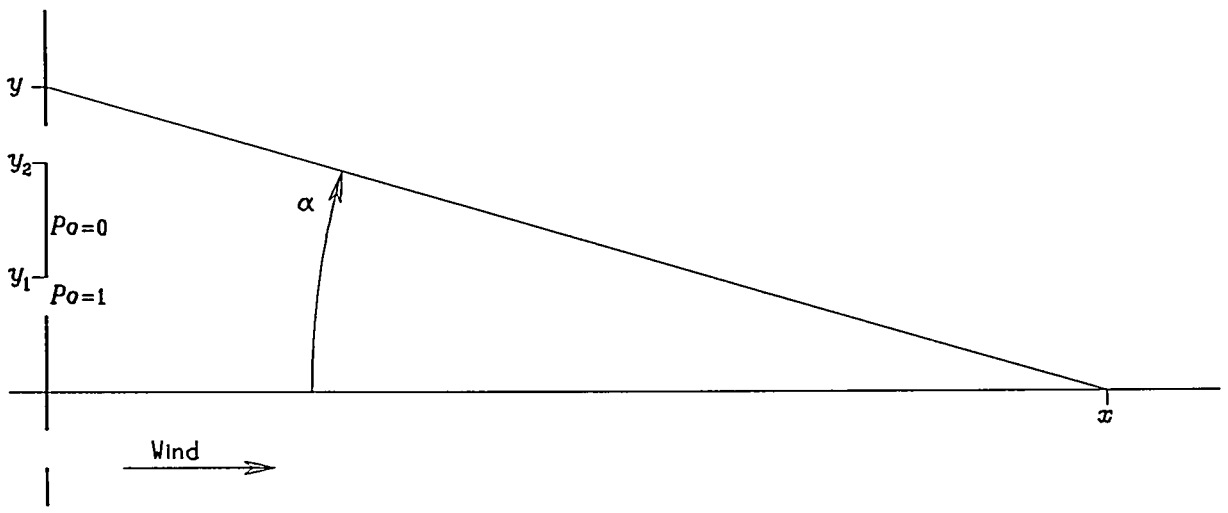

Figure 6. Finite length obstacles, for a distant point a single porous obstacle.

and taking the influence of a single finite length obstacle as

$$Pe_{\text{finite}} = G\, Pe_{\text{infinite}} \tag{57}$$

where the porosity used for the calculation of Pe_{infinite} is that of the finite length obstacle and where

$$G = \int_{y_1}^{y_2} f(x,y)\,dy = F(x,y_2) - F(x,y_1) \tag{58}$$

the sum over all the individual obstacles pieces equals at large distance that of a fence with a porosity close to the geometrical porosity of the interspaced obstacle: (space length)/(space+obstacle length).

A good choice for F and thereby for f is

$$F(x,y) = \int_0^y f(x,y)\,dy = \frac{1}{2}\tanh\left(A\frac{y}{x}\right) \tag{59}$$

$$f(x,y) = \frac{A}{2x}\left[1-\tanh^2\left(A\frac{y}{x}\right)\right] \tag{60}$$

As F is only a function of y/x, G becomes a function of y_1/x and b/x, where $b = y_2 - y_1$ is the length of the finite length obstacle.

The constant A is set so that the wake behind a finite length obstacle spreads in the same way as a free jet, i.e. the line through the points having half the velocity deficit of that at the wake centerline for same x, this line shall have an angle of 5 to 6 degree with the centerline. Figure 7 shows for a centrally positioned obstacle of length b the functions $G(x,y)$, and figure 8 shows $G(x,y)/G(x,0)$, i.e. the function relative to its centerline value. Due to the symmetry only half the plane is shown in these figures.

5.2 Equivalent 2D obstacles

The form of a "real" obstacle is like for old WAsP limited to a box with rectangular cross section, i.e. the input format only allows such obstacles.
The further limitation of the Perera formula and of the finite length function above, which only operates on 2-dimensional obstacles perpendicular to the wind, makes it necessary to replace the specified box with a set of 2D obstacles that

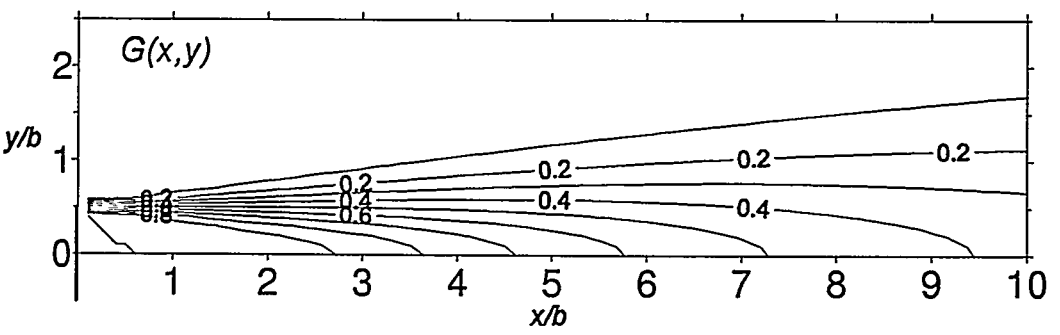

Figure 7. $G(x,y)$ as caused by an obstacle of length b.

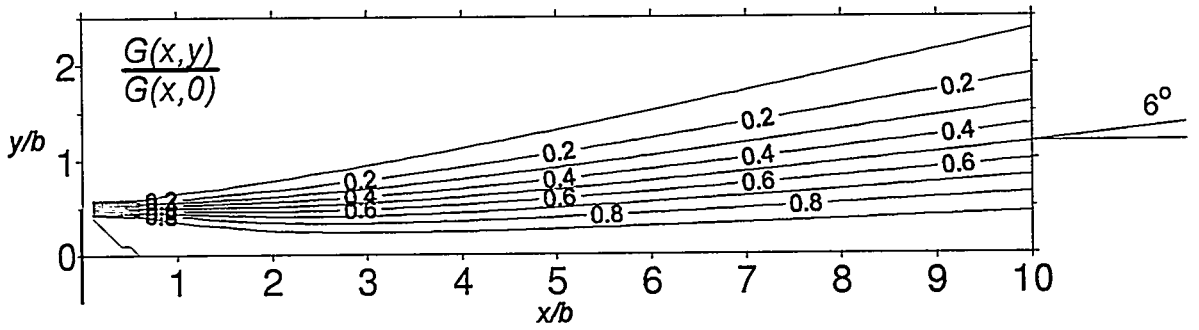

Figure 8. $G(x,y)/G(x,0)$ as caused by an obstacle of length b.

can be assumed to equivalent the box. This is accomplished by replacing the box with a number of 10 m or shorter 2D obstacles which are perpendicular to the wind and placed where the down wind sides of the real obstacle are specified. The thickness of the real obstacle is thereby disregarded.
Figure 9 shows a set of real obstacles and the equivalent 2D obstacles.

5.3 Influence of multiple obstacles

The influence of a multitude of obstacles upon a downstream point is assumed to be cumulative, i.e. the influence is the sum of influences of the individual obstacles, but so that an obstacle positioned downstream other obstacles has an effect in the point that corresponds to the reduced velocity at that obstacle as it is caused by the upstream obstacles.

With the obstacles ordered upstream downstream with number 1 being the most upstream the velocity at obstacle k is given by the recursion formula

$$U_k = U_{kf} - \Delta U_{kf} = U_{kf} - \sum_{j=1}^{k-1} U_j \, Pe_{jk} \, G_{jk} \tag{61}$$

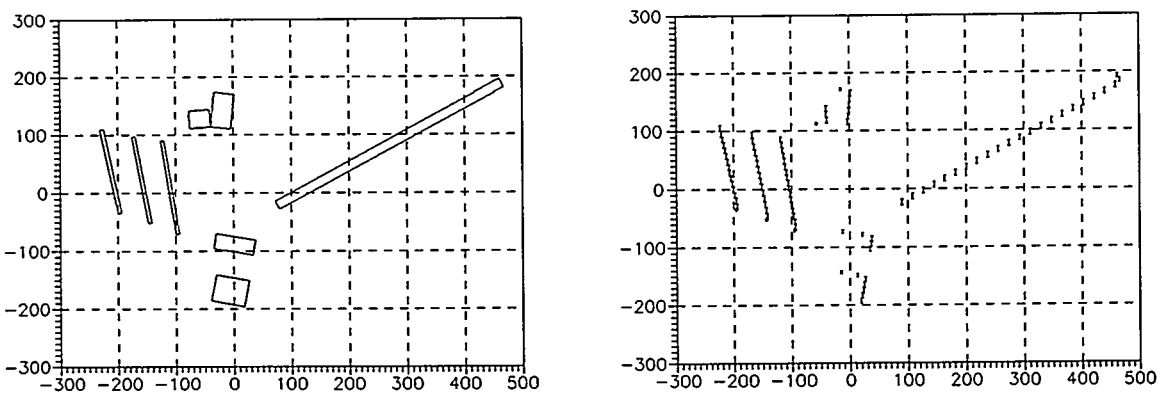

Figure 9. Left: Real obstacles. Right: Equivalent 2D obstacles for wind from the left. Dimensions in [m].

where now U is the velocity at top of the obstacle, subscripts j,k indicate individual obstacles, subscript f means free wind (without any obstacles), Pe_{jk} is Pereras formula for obstacle j and midpoint of obstacle k, and G_{jk} is likewise the geometrical factor for obstacle j and midpoint of obstacle k.
For a point p the formula is the same

$$U_p = U_{pf} - \Delta U_{pf} = U_{pf} - \sum_{j \text{ upstream } p} U_j \, Pe_{jp} \, G_{jp} \tag{62}$$

5.3.1 Closely spaced obstacles

If two equal size obstacles are being moved close to each other they should act as a single obstacle but partly due to the weakness of the Perera formula at small distances, partly due to the simple summation of deficits caused by the individual obstacles, they may rather behave as two individual obstacles giving a double speed reduction at the point of interest. To try to improve on this a function C – substituting G – is set up to reduce the direct influence of an obstacle at a downstream point, if other obstacles are present between the obstacle in question and the point. Whether this point is a so called "point of interest" or it is the midpoint of another obstacle makes no difference, except for the notation. Eqs. 61 and 62 then read:

$$U_k = U_{kf} - \sum_{j=1}^{k-1} U_j \, Pe_{jk} \, C_{jk} \tag{63}$$

$$U_p = U_{pf} - \sum_{j \text{ upstream } p} U_j \, Pe_{jp} \, C_{jp} \tag{64}$$

and the selected function reads for the two notations:

$$C_{ik} = \max\left(0, \left[G_{ik} - \sum_{j=i+1}^{k-1} G_{ji} \, G_{jk} \max\left(0, \, 1 - \frac{x_j - x_i}{5\,h_i + 2\,h_j}\right) \frac{h_j}{h_i} (1 - Po_j)\right]\right) \tag{65}$$

$$C_{ip} = \max\left(0, \left[G_{ip} - \sum_{j=i+1}^{\text{upstream } p} G_{ji} \, G_{jp} \max\left(0, \, 1 - \frac{x_j - x_i}{5\,h_i + 2\,h_j}\right) \frac{h_j}{h_i} (1 - Po_j)\right]\right) \tag{66}$$

Here $G_{ji,j>i}$, is the geometrical factor for obstacle j and the midpoint of obstacle i, i.e. as if the wind direction war reversed.
These functions give that obstacle j reduces obstacle i's influence at obstacle k, point p, if the obstacles are sufficiently close to each other: $x_j - x_i < 5h_i + 2h_j$, if obstacle j is not too porous and if it influences both upstream obstacle i and downstream obstacle k, point p.
In the case of two coinciding obstacles, the latter of zero porosity, G_{ji} becomes 1, and $G_{jk} = G_{ik}$ so C_{ik} becomes 0, i.e. obstacle i has no influence at obstacle k, while obstacle j has full influence, as i doesn't influence j when close enough, and so the two obstacles function as one.

5.3.2 Limits of influence

The influence of a 2D obstacle is strictly limited to the downstream side of that face of the rectangular obstacle it is a part of the equivalence for, see figure 10. 2D obstacles formed from the same real obstacle does not interact, i.e. $C_{ik} = 0$.

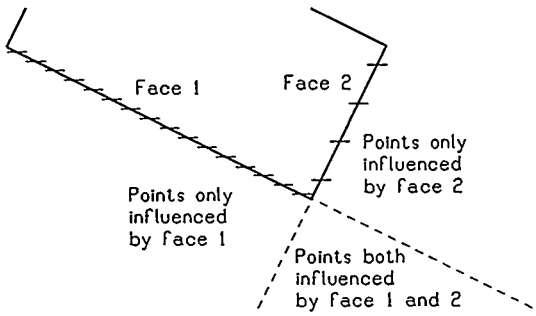

Figure 10. Space of influence of obstacle faces and equivalent 2D obstacles.

5.4 Roughness length

The Perera formula depends upon a single roughness length, a length that should be representative for the area in question.
The LINCOM model calculates a mean roughness for the total calculational area, but as this area may include both water stretches and land masses, the calculated mean roughness may not be representative for the area containing the obstacles. For the present obstacle model the needed roughness length is therefore taken as the geometric mean of the roughness found at the individual 2D obstacle equivalents:

$$z_{0,\text{mean}} = \exp\left[\frac{1}{N}\sum_{i=1}^{N}\ln z_{0,i}\right] \tag{67}$$

N being the number of equivalent 2D obstacles.

5.5 Free wind independence

For obstacle 1, the most upstream obstacle, $U_1 = U_{1f}$ per definition. As $U_{jf} \propto U_{1f}$ and the velocity deficit caused by an obstacle is proportional to the velocity at its top, all velocity deficits and thereby all velocities are proportional to U_1 for which reason the ratios U_j/U_{jf} and U_p/U_{pf} are independent of U_1, i.e. independent of the free wind speed.

5.6 Use within WAsP Engineering

The obstacle influenced velocities at the points of interest are found as the obstacle free velocities obtained with the LINCOM model multiplied with the free wind independent velocity ratios calculated with the obstacle model.

The position of the points of interest and their obstacle free velocities as well as the needed roughness information is read from LINCOM output files.

The obstacle position, size, and porosity is read from a WAsP obstacle file.

5.7 Test against obstacle model of WAsP

The described "Shelter" model has been compared to the obstacle model of WAsP for the case of "Waspdale Airport", a standard WAsP example. Figure 11 shows an air view of the obstacles with heights and porosities and a length scale indicated, and it shows the point and the twelve 30 degree wind direction sectors centered around 0, 30, 60, ..., 330 degree, for which WAsP gives a mean speed reduction. For two heights, 10 and 20 m, the predictions of the present model has been compared to the predictions of WAsP, figure 12. The results of the present model are given as continuous curves plus as the means over the 30 degree sectors – horizontal bars, the latter being directly comparable to the WAsP results, the crosses. As can be seen, the two models do not differ much. This is however no guarantee for correctness, but points to the common base, the Perera formula.

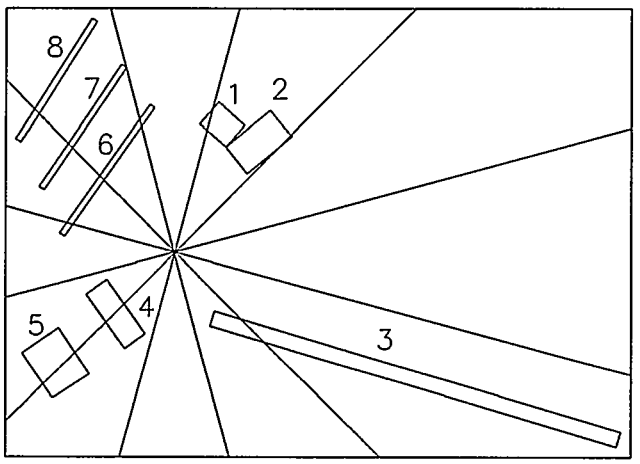

Obstacle	Height	Porosity
1	6 m	0.0
2	6 m	0.0
3	5 m	0.4
4	4 m	0.0
5	6 m	0.0
6	6 m	0.7
7	6 m	0.7
8	6 m	0.7

100 m

Figure 11. "Waspdale Airport" obstacles.

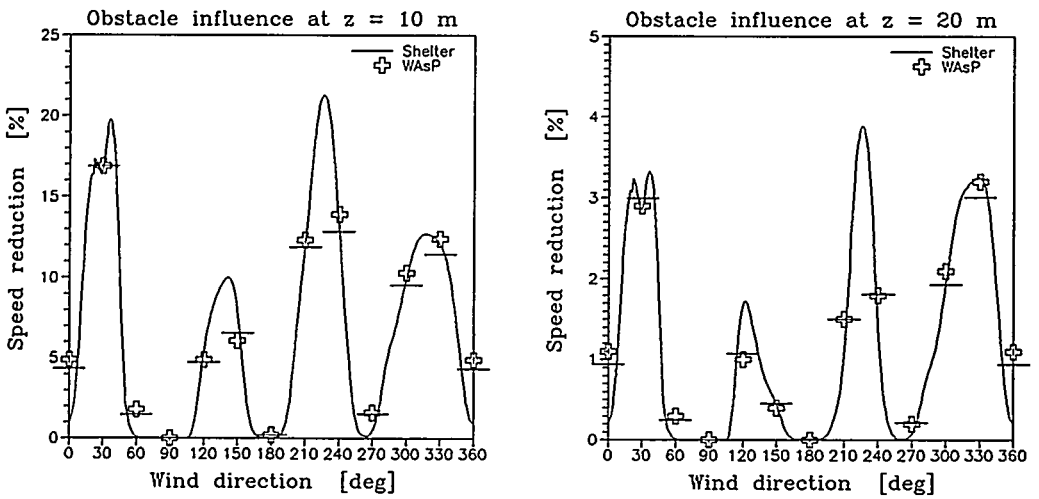

Figure 12. Comparison to obstacle model of WAsP. Continuous lines: present model; bars: present model mean over 30° sectors; crosses: WAsP 30° sector values.

6 Conclusion

The flow calculating and influencing models of WAsP Engineering have been described.

The model for sea surface roughness has been developed and interfaced in an iteratively manner with the LINCOM model for flow over terrain with hills and varying roughness.
More than wind the water roughness model needs water fetch, and to limit the influence of abruptly changing fetch perpendicular to the direction of wind, it has been necessary to smooth the calculated fetch.

The developed obstacle model is based on the Perera formula which seems to have a very limited range of application. This range has been widened by introducing some physics and a lot of thinking. It has been compared to the obstacle model of WAsP and gives results very near to the results of that model. Testing against experimental data is, however, the only way to find out how well it really works.

References

[1] Astrup, P.; Jensen, N.O.; and Mikkelsen, T. *Surface Roughness Model for LINCOM.* Risø-R-900(EN). Risø National Laboratory, Denmark, June 1996.

[2] Bradley, E.F. A micrometeorological study of velocity profiles and surface drag in the region modified by a change in surface roughness. *Quarterly Journal of the Royal Meteorological Society*, 94:361–379, 1968.

[3] Charnock, H. Wind stress over a water surface. *Quarterly Journal of the Royal Meteorological Society*, 81:639–640, 1955.

[4] Frank, H.P. 1996. Risø National Laboratory, Denmark. Personal communication.

[5] Hansen, C. and Larsen, S.E. Further work on the Kitaigorodskii roughness model length model: A new derivation using Lettau's expression on steep waves. *Geophysica*, 33(2):29–44, 1997.

[6] Hasselman, K.; Barnett, T.P.; Bouws, E.; Carlson, H.; Cartwright, D.E.; Enke, K.; Ewing, J.A.; Gienapp, H.; Hasselman, D.E.; Kruseman, P.; Meerburg, A.; Müller, P.; Olbers, D.J.; Richter, K.; Sell, W.; and Walden, H. Measurements of wind-wave growth and swell decay during the Joint North Sea Wave Project (JONSWAP). Deutsche Hydrografische Zeitschrift, Reihe A (8°), no. 12, Hamburg, 1973.

[7] Højstrup, J. Vand ruhed. 1997. Internal note. In Danish.

[8] Jackson, P.S. and Hunt, J.C.R. Turbulent wind flow over a low hill. *Quarterly Journal of the Royal Meteorological Society*, 101:929–955, 1975.

[9] Jensen, N.O.; Petersen, E.L.; and Troen, I. *Extrapolation of mean wind statistics with special regard to wind energy applications.* WCP–86. World Meteorological Organization, 1984. WMO/TD-No. 15.

[10] Johnson, H.K.; Højstrup, J.; Vedsted, H.J.; and Larsen, S.E. On the dependence of sea surface roughness on wind waves. *Journal of Physical Oceanography*, 1998. Accepted for publication.

[11] Landberg, Lars. *Short-term Prediction of Local Wind Conditions.* Risø-R-702. Risø National Laboratory, 1994. Ph.D. thesis.

[12] Lange, B. 1997. Personal communication.

[13] Mann, J. Modelling of the spectral velocity tensor in complex terrain. In: Larsen, A.; Larose, G.L.L.; and Livesey, F.M., editors, *Wind Engineering into the 21st Century. Vol. 1*, pages 257–264. A.A. Balkema, Rotterdam, 1999. Proceedings of the 10th International Conference on Wind Engineering, Copenhagen, Denmark, June 21–24, 1999.

[14] Perera, M.D.A.E.S. Shelter behind two-dimensional solid and porous fences. *Journal of Wind Engineering and Industrial Aerodynamics*, 8():93–104, 1981.

[15] Peterson, Ernest W.; Jensen, Niels Otto; and Højstrup, Jørgen. Observations of downwind development of wind speed and variance profiles at Bognaes and comparison with theory. *Quarterly Journal of the Royal Meteorological Society*, 105:521–529, 1979.

[16] Santabàrbara, J.M.; Mikkelsen, T.; Kamada, R.; Lai, G.; and Sempreviva, A.M. *LINCOM. Wind flow model.* Risø National Laboratory, Denmark, 1994. Not published.

[17] Toba, Y.; Iida, N.; Kawamura, H.; Ebuchi, N.; and Jones, I.S.F. Wave dependence of sea-surface wind stress. *Journal of Physical Oceanography*, 20:705–721, May 1990.

[18] Troen, Ib and de Baas, Anne. A spectral diagnostic model for wind flow simulation in complex terrain. In: *Proceedings of the European Wind Energy Association Conference & Exhibition*, pages 37–41. Rome, 1986.

Bibliographic Data Sheet Risø–R–1107(EN)

Title and author(s)

WAsP Engineering. Flow Model for Wind over Land and Sea

Poul Astrup and Søren E. Larsen

ISBN 87–550–2529–3

ISSN 0106–2840

Dept. or group
Wind Energy and Atmospheric Physics Department

Date
August 1999

Groups own reg. number(s)

Project/contract no.
ENS-1363/97-0004

Pages	Tables	Illustrations	References
24	0	12	18

Abstract (Max. 2000 char.)

This report presents the basic wind flow model of WAsP Engineering. The model consists in principle of three parts: the LINCOM model for neutrally stable flow over terrain with hills and varying surface roughness, a sea surface roughness model, and an obstacle model.

To better predict flow over or close to water bodies, the model for the sea surface roughness has been developed and interfaced with the existing LINCOM model. As the water roughness depends on the wind velocity, and the wind velocity on the roughness, the coupling is iterative.
The water roughness model is based on a fit to lots of literature data for the Charnock parameter as function of the so called wave age, the ratio between wave velocity and friction velocity, plus a correlation of wave age to the geometrically obtainable water fetch.

A model for the influence on the wind of multiple, finite size, interacting obstacles with any orientation has been formulated on the basis of the Perera formula for the influence of a single fence-like obstacle perpendicular to the wind. It is not a flow model but shall work as a postprocessor to the LINCOM model, which itself cannot treat such influence.

Descriptors INIS/EDB

COMPLEX TERRAIN; FLOW MODELS; ROUGHNESS; SEAS; W CODES; WIND

Available on request from Information Service Department, Risø National Laboratory,
(Afdelingen for Informationsservice, Forskningscenter Risø),
P.O. Box 49, DK–4000 Roskilde, Denmark
Phone +45 46 77 46 77, ext. 4004/4005 · Telex 43 116 · Telefax +45 46 77 40 13